Keyhole Formation During Spot Laser Welding. Heat and Fluid Flow Modeling in a 2D Axisymmetric Configuration

Mickael Courtois[*1], Muriel Carin[2], Philippe Le Masson[2] and Sadok Gaied[1]
[1]ArcelorMittal Global R&D Montataire France, [2]LIMATB Université de Bretagne-Sud Lorient France
[*]Corresponding author: mickael.courtois@univ-ubs.fr

Abstract : For a better understanding of physical phenomena associated to the appearance of defects in laser welding, a heat and fluid flow model is developed using Comsol Multiphysics®. This first step of the project is focused on the modeling of a static laser shot on a sample of steel. This 2D axial-symmetric configuration is used to study the main physical phenomena related to the creation of the keyhole. This model takes into account the three phases of the matter: the vaporized metal, the liquid phase and the solid base. To track the evolution of these three phases, coupled equations of energy and momentum are solved. The liquid / vapor interface is tracked using the Level-Set method. The calculated velocity and free surface deformation are analyzed. Melt pool shapes are compared to experimental macrographs and the influence of some parameters like laser power is discussed.

Keywords: Laser welding, keyhole, vapor, porosities, level-set, melt pool.

1. Introduction

Laser welded tailored blanks technology consist in assembling edge to edge, blanks of different thicknesses or different metallurgical properties. The goal is to obtain a ready to be stamped blank for automotive applications. The first advantage of this technology is to optimize the material and the thickness to the functional requirement. To a better understanding of this technology applied on very high strength steel, it is necessary to develop robust numerical model to predict the appearance of defect in the welded joint (Figure 1). These defects, like weld pool collapsing or partial penetration are present when the metal is in the liquid state and when the dynamic of solidification stop the form in an unwanted geometry. To predict the appearance of these defects a model of heat transfer and fluid mechanic is needed because they are first responsible of the final shape of the welded zone. Currently, 3D models able to simulate laser welding process are rare.

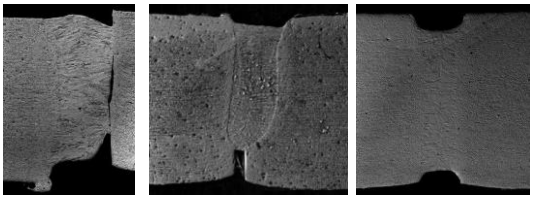

Figure 1 : Example of defects on tailored welded blanks (ArcelorMittal data)

2. Modeling of Laser welding process

1.1 Mains physical phenomena

During laser welding, the sheets to assembly are at the room temperature. The laser beam, with a radius of 500 µm, illuminates the surface sheet inducing the fusion of the zone to assembly. Because of very high energy density in laser, the material will be vaporized quickly. This vaporization will be accompanied by a recoil pressure, which will push the liquid, inducing a deformation and the appearance of the keyhole, a vapor capillary. The recoil pressure is the result of the vaporization by a phenomenon of action-reaction also called piston effect. This pressure is responsible for the digging and the maintenance of the keyhole. To realize the welded joint, the laser beam is moved at a speed of 3 to 20 m.min^{-1}. This speed is function of the laser power and the sheet metal thickness. In a steady state, three phases are present: the vapor in the capillary, the melt pool which flows around the keyhole with complex movements and finally the solid base away from the energy input (Figure 2).

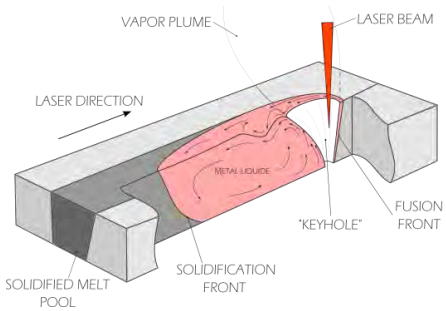

Figure 2 : Scheme of phenomena in laser welding

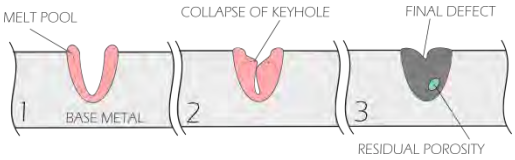

Figure 3 : Scheme of collapsing of the keyhole

The present goal is to take into account the vaporization of the steel and predict the location of the liquid-vapor interface using numerical method of front tracking. To keep an increasing difficulty, the first step is to suppose a static laser shot. This configuration with static source allows a 2D axisymmetric modeling as used by Medale [1] or Lee [2]. The goal is to predict, first, the correct kinetic of digging of the sheet and secondly the dynamics of melt pool collapsing (Figure 3). Although this configuration is apart from the industrial configuration, that is an essential step before a 3D configuration modeling. It is the better way to understand how modeling complex phenomena present and choose the better numerical method. The feasibility of a 3D modeling has been proved by Ki [3], Geiger [4], or Pang [5] with different calculation methods.

1.2 Mathematical formulation

For a heat and fluid flow modeling, it is necessary to solve conservation equations of energy (heat equation, Eq. 1), mass (continuity equation, Eq. 2) and momentum (Navier-Stokes, Eq. 3). The liquid metal is considered like an incompressible Newtonian under laminar flow.

$$\rho c_p \left[\frac{\partial T}{\partial t} + \vec{\nabla}.\left(\vec{u}\,T\right)\right] = \vec{\nabla}.\left(\lambda \vec{\nabla} T\right) + S \quad (1) \qquad \vec{\nabla}.\vec{u} = 0 \quad (2)$$

$$\rho\left(\frac{\partial \vec{u}}{\partial t} + \vec{u}.\left(\vec{\nabla}.\vec{u}\right)\right) = \vec{\nabla}.\left[-pI + \mu\left(\vec{\nabla}\vec{u} + \left(\vec{\nabla}\vec{u}\right)^T\right)\right] \quad (3)$$
$$-\rho\left(1-\beta\left(T-T_{melting}\right)\right)\vec{g} + \vec{F}_{Darcy} + \vec{F}_{ts}$$

With T the temperature, t the time, ρ the density, c_p the specific heat capacity, λ the thermal conductivity, S a heat source to represent the energy of the laser, $\vec{u}$ the velocity vector, p the pressure, I the identity matrix, μ the dynamic viscosity, $(.)^T$ the transposed matrix, $\vec{F}_{Darcy}$ a source term to cancel the velocity if the temperature is lower than the fusion temperature, $\vec{g}$ the gravity acceleration and $\vec{F}_{ts}$ the normal and tangential force vector from the effects of surface tension. The surface tension coefficient is assumed constant in this model witch involves that the Marangoni effect is neglected.

Conservation equations are solved in the three phases (vapor, liquid and solid) and a front tracking method is added to the model. The method chosen to track the liquid gas interface is the Level-Set method [6]. This method used a fixed mesh and defines a variable Φ in the entire computation domain. This variable takes the value of 1 in the vapor phase and 0 in the liquid (and solid) phase. With this method it is easy to define different properties in each phase and the interface is identified by locating the isovalue Φ=0.5. The movement of the liquid/gas interface is realized by advecting the Φ variable using the velocity field calculation. Near the interface, the Φ variable varies progressively with a smooth step function, inducing the properties variation from a phase to the other (Figure 4a). The thickness of this transition must be defined with caution to be close to the reality but in avoiding numerical convergence problems. Nevertheless the Level-Set method has the main advantage of treated the complex geometric change of the interface. So, it is possible to simulate the formation of porosity and the transition from partial to full penetration mode.

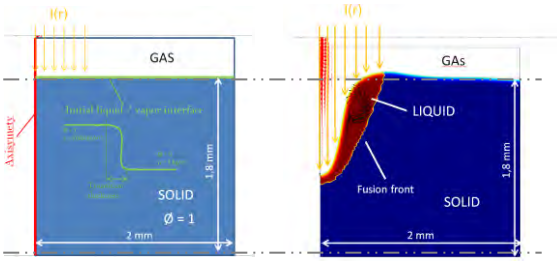

Figure 4a : Initial geometry and variable Φ

Figure 4b : Deformed geometry at t = 20 ms

With the Level-Set method, the boundary conditions of the interface are in the calculation domain. These conditions are implemented like source terms in conservation equations using to the Φ variable position. So, the laser energy is deposed at the surface of the metal by the source term in the heat equation. It is supposed as a Gaussian distribution (Eq. 4):

$$I(r) = \frac{P_{max}}{\pi R_g^2}\exp\left(\frac{-r^2}{R_g^2}\right)\delta_z(\phi) \quad (4)$$

With P_{max} the laser power, R_g the radius of the Gaussian distribution and δ_z a Dirac function to apply the energy only at the surface of the liquid. The vaporization resulting from this energy induces a recoil pressure at the origin of the creation of the capillary. This pressure imposes a "piston effect" to the underlying material. So, the melt pool directly under the vaporization layer is moved and ascends on the sides to form rolls at the surface (Figure 3).
Generally, the recoil pressure is applied using an empirical formulation [2, 4, 5]. So this is

not resulting from the calculation. A way more physical is to introduce a source term in the continuity equation. It will be non-zero only on the interface (Eq. 5). Indeed, incompressibility of fluid phases is not satisfied near the interface because of the density difference on the both sides of the interface in gaseous phase (ρ_v) and liquid phase (ρ_l). For the same reason, the Level Set transport equation (Eq. 6) is also modified with the same method. These source terms create an evaporation flow rate $\dot{m}$ (Eq. 7) which is deduced mainly from the local temperature and the saturated vapor pressure [8].

$$\vec{\nabla}.\vec{u} = \dot{m}\,\delta(\phi)\left(\frac{\rho_l - \rho_v}{\rho^2}\right) \quad (5)$$

$$\frac{\partial\phi}{\partial t} + \vec{u}.\vec{\nabla}\phi - \dot{m}\,\delta(\phi)\left(\frac{f_l}{\rho_l} + \frac{f_v}{\rho_v}\right) = 0 \quad (6)$$

$$\dot{m} = \sqrt{\frac{m}{2\,\pi\,k_b}}\,\frac{p_{sat}(T)}{\sqrt{T}}\left(1-\beta_r\right) \quad (7)$$

With f_l and f_v the relative fraction of liquid and vapor between 0 and 1, m the atomic weight of iron, k_b the Boltzmann constant, $p_{sat}(T)$ the saturated vapor pressure, and β_r the retro-diffusion coefficient supposed equal to 0 in a first approximation.

2. Numerical results

The previous equations are solved in a 2D axisymmetric configuration with the finite elements code COMSOL Multiphysics®. The simulation correspond to a laser shot of 25 ms followed by 5 ms of cooling. The focal spot diameter is 600 µm and the sample is a disk of 2 mm of radius and 1.8 mm of thickness. The material properties are given in the following table I:

$\rho_l = 7000$ kg.m^{-3}	$\lambda_l = 40$ W.m^{-1}.K^{-1}	$c_{pl} = 400$ J.kg^{-1}.K^{-1}	$\mu_l = 5.10^{-3}$ Pa.s^{-1}	$\sigma = 1{,}5.10^{-1}$ N.m^{-1}
$\rho_v = 10$ kg.m^{-3}	$\lambda_v = 10$ W.m^{-1}.K^{-1}	$c_{pv} = 1000$ J.kg^{-1}.K^{-1}	$\mu_v = 1.10^{-5}$ Pa.s^{-1}	

Table I : Thermophysical properties of the liquid and vapor phases

The figure 4 illustrates the deformation of the melt pool under the effect of the recoil pressure and shows the appearance of the vapor capillary. This approach using a source term in the continuity equation produces more realistic velocity fields in the vapor phase than the one using an empirical formulation for the recoil pressure. Indeed, in this case, the addition of the source term generates a vapor flow rate near the interface affecting the velocity field in the vapor phase. When the recoil pressure is calculated with an empirical low, the velocities in the vapor phase are only a result of the displacement of the liquid vapor interface, so the interaction between vapor jet and the melt pool can not be represented correctly. However, this interaction has a significant impact on the shapes of the welded join, as shown by high speed camera observation [9, 10]. Indeed, in the presence of high welding speeds, the front edge of the capillary vapor undergoes an inclination. The laser beam impacts the forward front resulting in a stronger evaporation at this front. This vapor jet interacts strongly with the back of the melt pool and can cause the phenomenon of "humping", a formation of bumps at the surface of the melt pool. Note, however, that in the 2D axisymmetric configuration used here, the interaction between vapor jet and the liquid remains very limited because the vapor jet is mainly directed upwards.

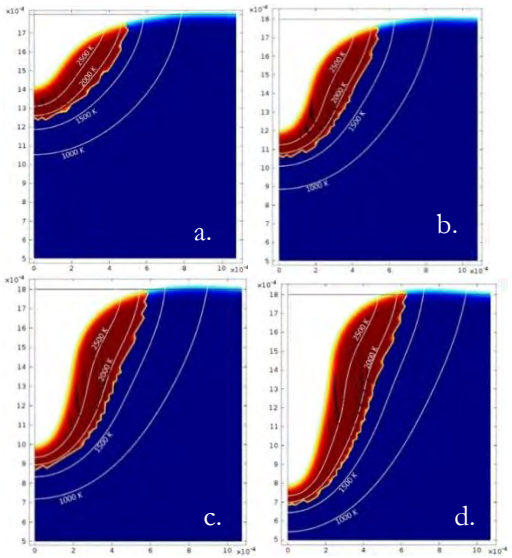

Figure 5 : Melt pool shapes and isotherms for different laser powers :

a. P = 400 W, b. P = 500 W, c. P = 600 W, d. P = 700 W at t = 20 ms

To illustrate the laser power influence on the digging of the liquid surface, the figure 5 presents melt pool shapes and isotherm for varying power from 400 to 700 W for a shot of 20 ms. We can observe that temperature levels increasing with laser power, resulting in a more intense vaporization phenomenon. A greater penetration is then observed with a more vertical inclination of the liquid surface that can lead to instabilities.

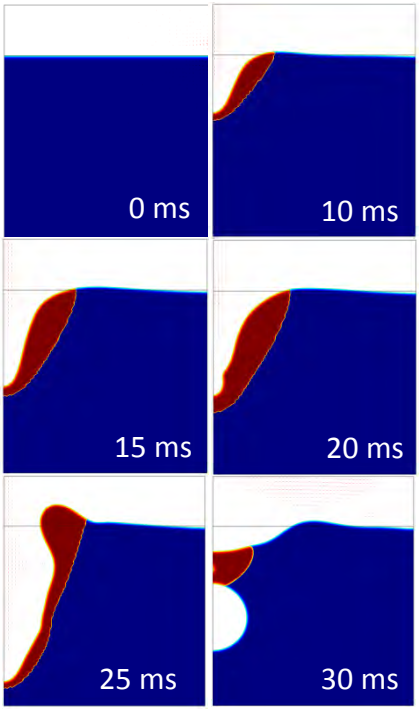

Figure 6 : Porosity formation during the keyhole collapse process. Melt pool shapes with 25 ms of heating and 5 ms of cooling (Laser power = 900W)

It has been shown by many authors [9, 10] that the inclination of the liquid surface increases with the laser power. At high laser power the model presents a different mechanism of collapsing of the melt pool during the cooling. When the laser irradiation is shut off, vaporization and so recoil pressure are immediately stopped. The gravity and the surface tension are the only force acting and lead to the collapse of the keyhole. If the keyhole is sufficiently deep, a gas cavity is formed during collapse. Theses residual porosities are observed experimentally and the model helps the understanding of their formation.

3. Experimental study

A series of experiments was performed at PIMM to approach two goals. The first one is to obtain a transient evolution of welded zone geometry to validate the numerical model. The second is to identify the operating conditions leading, or not, to the formation of residual porosities. To achieve these goals, a series of static shots were realized by varying the laser power and time of interaction of the laser. The laser used is a disk laser type Nd:YAG (λ = 1.06 µm). The diameter of the focal spot is fixed to 600 µm. Shots are operated on DP 600 steel samples with a thickness of 1.8 mm. Cross-section macrographs after chemical etching (Béchet-Beaujard) were performed in order to measure the melt pool size evolution.

Figure 6a shows macrographs for a laser power of 1000W with an interaction time varying from 2 to 25 ms. No porosity is observed at low power. The melt pool shape is like a bowl, whereas at a power of 1500 W (Figure 7b), the profile of melted zone is narrower. At high laser powers, we can notice the presence of residual porosities sometimes. Some porosity can appear at the very beginning of laser irradiation. The figure 7b illustrates, for an interaction time of 6 ms, porosity very close to the base metal. This indicates, because of a high energy density, a very high recoil pressure dominating all other forces in. Under these conditions, the liquid is removed very quickly on the sides and it is ejected upward. During the presence of the keyhole, there are temporary areas where the liquid layer is extremely thin, the vapor is here almost in contact of the solid. Note that at high power, the liquid has probably not a stable position. Under the effect of recoil pressure, the melt pool is ejected then it collapses on itself. Irradiation continuing, it is immediately chased and repeatedly. These successions of collapsing and repulsion can be extremely fast, up to create a corrugated surface. When the laser is stopped, keyhole is collapsing capturing sometimes gas cavity. For a power of 1500 W, porosity are present on more than 50% of shots. This rate drops to less than 10% for a power of 1000 W. However, we have seen with the numerical model, more the power is elevated, more the inclination of the liquid boundary is steep. This phenomenon favors the concentration of energy in the bottom of keyhole because of laser reflections, and favors the formation of porosity during the keyhole collapse process. This analysis is in agreement with the experimental observations of Girard and al [11], which have shown that the appearance of porosity is due to two factors: the keyhole shape and the solidification time.

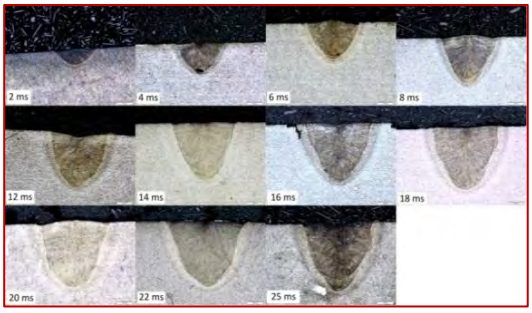

Figure 7a : Macrographs of fusion zones; variable interaction time ; P_{laser} = 1000W

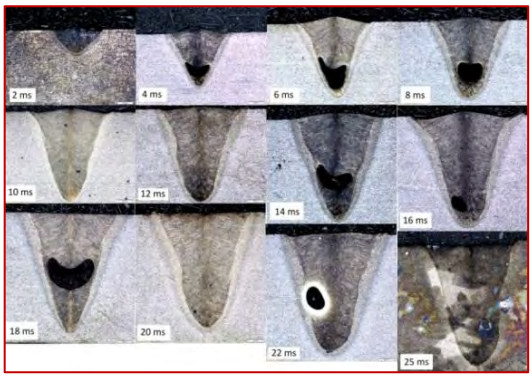

Figure 7b : Macrographs of fusion zones; variable interaction time ; P_{laser} = 1500W

The figure 8a shows that the penetration depth for powers of 1000 and 1500 W, increases quickly without stabilization at 25 ms. The width, begins to stabilize at around 16 ms of laser irradiation. Indeed, the focal spot diameter is limited and energy will concentrate at the bottom of the keyhole increasing the depth rather than the side diffusion. Note that the numerical model predicts with a good agreement depth penetration with however an overestimated width of melted zone. Considering the assumptions made, the global temporal evolution is satisfactory.

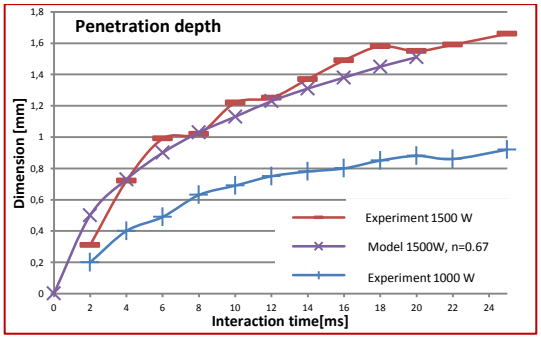

Figure 8a : Time evolution of penetration depth ; Experiment and numerical results

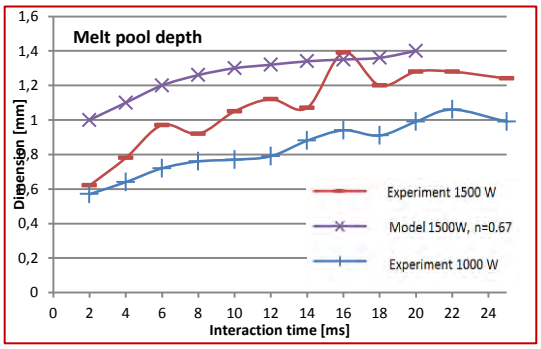

Figure 8b : Time evolution of melt pool width ; Experiment and numerical results

5. Conclusion and outlook

A 2D axisymmetric heat transfer and fluid flow model has been developed to simulate the keyhole formation under a laser irradiation. This model takes into account multiple phenomena like fusion evaporation, surface tension, gravity and calculates temperature, pressure and velocity fields in liquid and gaseous phases. The model gives also the deformation of the liquid surface due to the recoil pressure.

Using the Level-Set method, the calculated results are consistent with experimental observations. The development of an original method, more complex but more physical, to take into account the recoil pressure consists in introducing the evaporation mass flow rate in mass conservation equation. With this method, the phase change from liquid to vapor can be observed and the interaction between vapor jet and the liquid surface can be analyzed.

An experimental study was performed to identify operating conditions leading or not to the appearance of defects like residual porosity. For a laser power greater than 1000 W, the violent ejection of liquid has been demonstrated with postmortem cross-section macrographs, showing residual porosity. The macrograph analysis has also indicated that, the liquid thickness can be very thin. At last, increasing laser power, leads to melted zones narrower, due to a deeper keyhole, liquid wall steeper and so a greater concentration of energy at the bottom of the cavity gas.

The next step of this work is to compare in detail the digging dynamics measured and calculated by the model. To improve the model, rays multiple reflections on the keyhole surface should be considered. In the longer term, the goal is to extend 2D axisymmetric case to the three dimensional industrial case with advance of the laser. The final goal is to propose a model able to predict the appearance of defects for a set of welding parameters given in three dimensions.

6. References

[1] M. Medale, C. Xhaard, R. Fabbro, "A thermo-hydraulic numerical model to study spot laser welding", *C. R. Mecanique 335* (2007), 280-286

[2] J. Lee, S. Ko, D. Farson, C. Yoo, "Mechanism of keyhole formation and stability in stationary laser welding", *J. Phys. D : Appl. Phys. 35* (2002), 1570-1576

[3] H. Ki, P. Mohanty, J. Mazumder, "Modeling of laser keyhole welding: Part I. Mathematical modeling, numerical methodology, role of recoil pressure; multiples reflections and free surface evolution", *Metall. Mater. Trans A 33A* (2002), 1817-1830

[4] M. Geiger, K.H. Leitz, H. Koch, A. Otto, "A 3D transient model of keyhole and melt pool dynamics in laser beam welding applied to the joining of zinc coated sheets", *Prod. Eng. Res. Devel.* (2009), 3 :127-136

[5] S. Pang, L. Chen, J. Zhou, Y. Yin, T. Chen, "A three-dimensional sharp interface model for self-consistent keyhole and weld pool dynamics in deep penetration laser welding", *J. Phys. D : Appl. Phys. 44* (2011)

[6] S. Osher and J. A. Sethian, "Fronts propagating with curvature dependent speed: algorithms based on Hamilton-Jacobi formulations", *J. Comput. Phys. 79* (1988), 12-49

[7] A. Esmaeeli, "Computations of film boiling. Part I: numerical method", *Int. J. Heat Mass Trans. 47* (2004), 5451-5461

[8] C. Mas, "Modélisation physique du procédé de découpe de métaux par laser", Thèse de doctorat, Université de Paris 6, 2003

[9] K. Chouf, "Etude du comportement du capillaire en régime de soudage laser forte pénétration", Thèse de doctorat, Université de Paris XIII, 2002

[10] R. Fabbro, S. Slimani, F. Coste, F. Briand, "Analysis of the various melt pool hydrodynamic regimes observed during CW Nd-YAG penetration laser welding", *ICALEO Conference 2007*, Orlando, USA

[11] K. Girard, J. Jouvard, Ph. Naudy, "Study of voluminal defects observed in laser spot welding of tantalum", *J. Phys. D: Appl. Phys. 33 (2000) 2815-2824*

9. Acknowledgements

The authors are grateful to Professor Patrice Peyre and Rémy Fabbro from PIMM laboratory (ENSAM, Paris) to their support for our experimental investigations.